A Robust Adaptive Controller for Surface-Mount Permanent Magnet Synchronous Machines

David M. Reed, Jing Sun, and Heath F. Hofmann

Abstract— **High torque density and the potential for high efficiency have made Surface-Mount Permanent Magnet machines an attractive option for many high performance drive applications. However, parameter variations due to temperature changes, skin effect, and magnetic saturation, can detune the transient characteristics of the drive, and cause large mismatches in torque regulation. The approach presented in this paper utilizes a combination of adaptively tuned feedforward and feedback-decoupling terms, in addition to standard proportional feedback for added robustness. The resulting controller achieves consistent transient response characteristics with zero steady-state error over a wide range of operating points, without the use of integral control. The adaptive law is derived using Lyapunov's stability theorem, and the resulting adaptive controller is tested numerically in Simulink. Experimental results confirm the performance of the proposed adaptive controller.**

I. Introduction

The Surface-Mount Permanent Magnet (SMPM) machine has become a popular choice for many drive applications, due to its high torque density and potential for high efficiency. However, variations in machine parameters due to temperature changes, skin effect, and saturation can detune the transient characteristics of the drive, and cause significant steady-state errors in regulated torque. Temperature variations primarily impact the stator resistance, which can increase by as much as 100% [1], and permanent magnet flux, which has a negative temperature coefficient of around 0.1% per °C for neodymium ($NdFeB$) magnets [2]. In the case of high-pole-pair designs and high-speed applications, the electrical frequencies in the stator can reach levels where skin effect begins to cause a noticeable increase in stator resistance. This paper presents a robust adaptive field-oriented control (FOC) strategy which allows for simultaneous identification and torque regulation in SMPM machines with slowly-varying parameters.

Field-oriented control [3] and its variants have become the standard for high-performance control of AC machinery and drive systems. By projecting the sinusoidal electrical variables into appropriate rotating reference frames using the Park transform [4], a decoupling of the torque and field generating components of electrical currents is achieved. The resulting field-oriented machine dynamics constitute an overactuated system whose control is analogous to that of a separately excited (field-winding) DC machine, where field and torque generating electrical currents are independently controlled. Furthermore, electrical variables which are sinusoidal in the stationary reference frame are constant in field-oriented frames, allowing the use of conventional PI current regulators. While FOC offers a number of advantages over other control strategies for AC machines, the technique also suffers from well known sensitivities to parameter variations.

A variety of approaches have been proposed by researchers to address the issue of parameter variation in Permanent Magnet Synchronous Machines (PMSMs). Least square estimators (LSEs) have been designed for the purpose of estimating machine parameters online in closed-loop [5], [6], and open-loop [7] configurations. The approach presented in [5] divides the estimation task into a "fast" LSE for the inductances, and a separate "slow" LSE for resistance and torque constant which are functions of slow thermal variations. In [8], the author uses the gradient (steepest descent) algorithm to adaptively estimate parameter variations, which are modeled as lumped time-varying disturbances. Another approach to online adaptation is the use of artificial neural networks [9]. Still, Lyapunov-based designs are an attractive approach as they provide some stability assurances as part of the design process [10]. To avoid some of the complexity associated with parameter estimation based on dynamic models, the authors of [11] and [12] develop their parameter estimators using steady-state machine models.

This paper presents a new robust adaptive torque regulating controller for SMPM machines which estimates resistance, inductance, and permanent magnet flux linkage online. The adaptive controller to be presented is derived using Lyapunov's stability theorem, and so the stability of the closed-loop system is demonstrated in the process of deriving the adaptation law. A robust modification to the derived adaptive law is used to ensure closed-loop stability in the presence of unmodeled disturbances. The control law utilizes a combination of adaptively-tuned feedforward (to achieve zero steady-state error), $d-q$ decoupling (to improve transient response), and proportional feedback (to add robustness to disturbances) terms. Overactuation of the system is exploited to simultaneously achieve parameter convergence and torque regulation. After reviewing the dynamic SMPM machine model, the derivation and stability proof for the proposed adaptive controller is presented. Simulation results verifying the performance of the control design are presented. Finally, some remarks specific to experimental implementation challenges, as well as experimental results, are discussed.

David M. Reed and Heath F. Hofmann are with the department of Electrical Engineering and Computer Science and Jing Sun is with the department of Naval Architecture and Marine Engineering at the University of Michigan, Ann Arbor, MI 48109 USA (e-mail: davereed@umich.edu; jingsun@umich.edu; hofmann@umich.edu).

This work was sponsored by the U.S. Office of Naval Research (ONR) under Grants No. 00014-11-1-0831 and U.S. Navy through the Naval Engineering Education Center (NEEC).

Preprint submitted to 2014 American Control Conference.
Received September 27, 2013.

TABLE I
LIST OF NOTATION AND SPECIAL MATRICES.

Symbol	Description
Electrical Variables	
$\vec{v}(t)$	Stator Voltage Vector
$\vec{i}(t)$	Stator Current Vector
$\vec{\lambda}_{PM}$	Permanent Magnet Flux Linkage Vector
R	Stator Winding Resistance
L	Stator Self-Inductance
Λ_{PM}	Permanent Magnet Flux Linkage
Mechanical Variables	
τ_{3ph}	Three-Phase Electromagnetic Torque
ω_r	Rotor Angular Velocity
ω_{re}	Rotor Electrical Angular Velocity
P	Number of Poles
Special Matrices	
$\mathbf{J} = \begin{bmatrix} 0 & -1 \\ 1 & 0 \end{bmatrix}$	90° Rotation Matrix
$e^{-\mathbf{J}\theta}$	Park Transform (Arbitrary Rotation Matrix)

II. SMPM MACHINE MODEL

A. Machine Dynamics in the Rotor Reference Frame

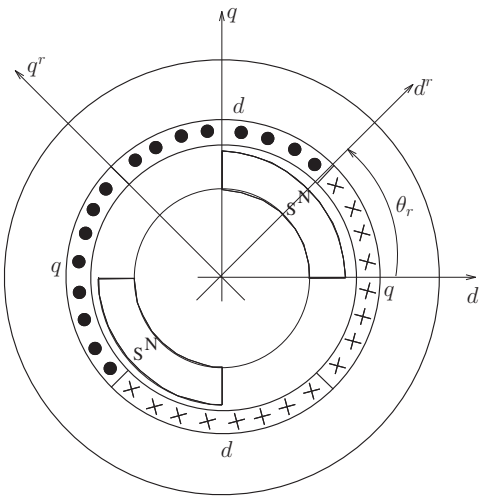

Fig. 1. Cross-section of the two-phase equivalent, two-pole smooth airgap SMPM machine.

The proposed control algorithm is designed around the standard two-phase equivalent model for SMPM machines (Fig. 1). This model and subsequent control design assumes the following:

- **A1.** The machine to be controlled has a smooth airgap (i.e., slotting effects are neglected), is fed by an ideal voltage source inverter (VSI), and is balanced in its construction such that it can be accurately represented by its 2-phase equivalent.
- **A2.** Saturation and core loss are neglected, and it is assumed that any magnetic saliency is negligible (i.e., $L_d = L_q = L$).
- **A3.** The rotor and mechanical load have enough inertia that a significant time-scale separation exists between electrical and mechanical dynamics.
- **A4.** The sampling frequency of the digital implementation is high enough that a continuous-time control design can be sufficiently approximated.
- **A5.** Accurate measurements of the stator currents, rotor position and rotor velocity are available. Stator voltage and torque are not measured.

These assumptions are typical and valid under normal operation. The first three assumptions (**A1** - **A3**) simplify the model by reducing its order and maintaining linearity. The last two assumptions (**A4** and **A5**) pertain to the control design and methodology.

Transformed into the rotor reference frame, which is denoted by a superscript "r", the electrical dynamics take the form,

$$L\frac{d\vec{i}^r}{dt} = -R\vec{i}^r - \omega_{re}\mathbf{J}\left(L\vec{i}^r + \vec{\lambda}^r_{PM}\right) + \vec{v}^r \qquad (1)$$

where $\vec{i}^r = \begin{bmatrix} i^r_d & i^r_q \end{bmatrix}^T$ is the state vector containing the "direct" and "quadrature" stator currents, $\vec{v}^r = \begin{bmatrix} v^r_d & v^r_q \end{bmatrix}^T$ is the control input vector of stator voltages, $\vec{\lambda}^r_{PM} = \begin{bmatrix} \Lambda_{PM} & 0 \end{bmatrix}^T$ is the permanent magnet flux linkage vector, R is the stator resistance, L is the stator self-inductance, and ω_{re} is the rotor electrical frequency (i.e., $\omega_{re} = \frac{P}{2}\omega_r$, where P is the number of poles and ω_r is the mechanical rotor frequency). In the rotor reference frame, the electromagnetic torque is given by,

$$\tau_{3ph} = \frac{3P}{4}\Lambda_{PM} i^r_q. \qquad (2)$$

Finally, the separation between the electrical and mechanical time constants is roughly a factor of 150. Therefore, the rotor speed is treated as a known constant with respect to the electrical dynamics (1), as there exists a significant time-scale separation between the electrical and mechanical dynamics to justify **A3**.

B. Test Machine Parameters

For simulation and comparison purposes, the parameters of the SMPM test machine from MOTORSOLVER were measured and/or estimated using standard techniques. The stator resistance was measured with a Digital Multi-Meter, inductance with an Agilent E4980A LCR meter, and the permanent magnet flux linkage was identified using the "open circuit test" and a linear regression. These "assumed" parameters, denoted by an "overbar" ($\bar{}$), are provided in Table II.

III. ADAPTIVE CONTROL DESIGN

A. Statement of Control Objective

The control objective is the accurate regulation of electromagnetic torque in SMPM machines, over a wide range of operating conditions. This is accomplished through the design of an adaptive torque-regulating controller which is

Preprint submitted to 2014 American Control Conference.
Received September 27, 2013.

TABLE II
ASSUMED TEST MACHINE PARAMETERS.

Parameter	Value
Resistance, $\bar{R}$	102.8 mΩ
Self-Inductance, $\bar{L}$	212.3 μH
PM Flux Linkage, $\bar{\Lambda}_{PM}$	12.644 mV-s
No. of Poles, P	10

capable of tracking torque commands with zero steady-state error in the presence of slowy-varying, uncertain parameters. A Persistently Exciting (PE) direct-axis stator current is commanded to aid parameter convergence over a wide operating range, while decoupling is employed to ensure that the PE signal does not induce ripple in the quadrature-axis stator current, which would induce unwanted ripple in the generated torque.

B. Adaptive Control Algorithm Derivation

The relationship between torque, which is unmeasured, and quadrature current in (2) suggests that torque regulation is achievable by regulating the quadrature-axis stator current i_q^r, which is easily measured. Furthermore, (1) suggests that the stator currents (i.e., the system states) can be regulated by applying appropriate stator voltages (i.e., the control inputs). The stator current error vector is defined as follows:

$$\vec{e}_i^{\,r} = \tilde{\vec{i}}^r - \vec{i}^r, \tag{3}$$

where the "tilde" ($\tilde{}$) is used to denote a reference value. The following control law,

$$\vec{v}^r = \hat{R}\tilde{\vec{i}}^r + \omega_{re}\mathbf{J}\hat{\vec{\lambda}}_{PM}^r + \hat{L}\frac{d}{dt}\tilde{\vec{i}}^r + \hat{L}\left(\omega_{re}\mathbf{J}\vec{i}^r + K_p\vec{e}_i^{\,r}\right), \tag{4}$$

is formulated using a combination of feedforward, feedback, and decoupling terms, designed to yield exponentially stable stator current error dynamics (5) under perfect model knowledge (i.e., $\hat{R} = R$, $\hat{L} = L$, and $\hat{\vec{\lambda}}_{PM}^r = \vec{\lambda}_{PM}^r$):

$$\frac{d}{dt}\vec{e}_i^{\,r} = -\left(\frac{R}{L} + K_p\right)\vec{e}_i^{\,r}, \tag{5}$$

where the "hat" ($\hat{}$) is used to denote an estimated value, and $K_p > 0$ is a constant proportional control gain. However, when the parameters R, L, and $\vec{\lambda}_{PM}^r$ are not well known, one can show that the closed-loop error dynamics satisfy the following equation:

$$\begin{aligned}\frac{d}{dt}\vec{e}_i^{\,r} = &-\left(\frac{R}{L} + K_p\right)\vec{e}_i^{\,r} + \frac{e_R}{L}\tilde{\vec{i}}^r + \frac{\omega_{re}}{L}\mathbf{J}\vec{e}_{\lambda_{PM}} \\ &+ \frac{e_L}{L}\left(\frac{d}{dt}\tilde{\vec{i}}^r + K_p\vec{e}_i^{\,r} + \omega_{re}\mathbf{J}\vec{i}^r\right),\end{aligned} \tag{6}$$

where, $e_R = R - \hat{R}$, $e_L = L - \hat{L}$, and $\vec{e}_{\lambda_{PM}} = \vec{\lambda}_{PM}^r - \hat{\vec{\lambda}}_{PM}^r = \begin{bmatrix} e_\Lambda & 0 \end{bmatrix}^T$. To stabilize (6) and achieve the control objectives, adaptation is required to adjust the values of $\hat{R}$, $\hat{L}$, and $\hat{\Lambda}_{PM}$. A block diagram of the proposed controller implementation is given in Fig. 2, where the crossing arrows behind blocks symbolize portions of the controller which are tuned by the adaptation. Note that in practice, implementation of the control law (4) uses filtered commands (i.e., $\tilde{\vec{i}}^r = \{M(s)\}\,\vec{i}_{cmd}^{\,r}$ and $\frac{d}{dt}\tilde{\vec{i}}^r = \{sM(s)\}\,\vec{i}_{cmd}^{\,r}$, where $M(s)$ is a stable first-order transfer function)[1] to prevent feeding forward an unbounded signal during a step-change in references.

To derive the adaptive update law, a Lyapunov stability analysis of the closed-loop system is first performed. The adaptive law is then chosen such that it makes the Lyapunov function monotonically decreasing, thereby guaranteeing closed-loop stability of the controlled system. The following Lyapunov function candidate forms the basis of the derivation:

$$V(\vec{e}_i^{\,r}, \vec{e}_\theta) = \frac{1}{2}\left(\vec{e}_i^{\,rT}\vec{e}_i^{\,r} + \frac{1}{L}\vec{e}_\theta{}^T\mathbf{\Gamma}^{-1}\vec{e}_\theta\right), \tag{7}$$

where $\mathbf{\Gamma} = \mathbf{\Gamma}^T > 0$ is the adaptation gain, and $\vec{e}_\theta = \begin{bmatrix} e_R & e_L & e_\Lambda \end{bmatrix}^T$. The first derivative of (7) with respect to time is given by,

$$\dot{V}(\vec{e}_i^{\,r}, \vec{e}_\theta) = \vec{e}_i^{\,rT}\dot{\vec{e}}_i^{\,r} + \frac{1}{L}\vec{e}_\theta{}^T\mathbf{\Gamma}^{-1}\dot{\vec{e}}_\theta. \tag{8}$$

Substituting (6) into (8), with some manipulation, yields,

$$\begin{aligned}\dot{V}(\vec{e}_i^{\,r}, \vec{e}_\theta) = &-\left(\frac{R}{L} + K_p\right)\vec{e}_i^{\,rT}\vec{e}_i^{\,r} \\ &+ \frac{1}{L}\vec{e}_\theta^{\,T}\mathbf{\Phi}^T\vec{e}_i^{\,r} + \frac{1}{L}\vec{e}_\theta\mathbf{\Gamma}^{-1}\dot{\vec{e}}_\theta\end{aligned} \tag{9}$$

where

$$\begin{aligned}\mathbf{\Phi} &= \left[\begin{array}{c|c|c} \tilde{\vec{i}}^r & K_p\vec{e}_i^{\,r} + \frac{d}{dt}\tilde{\vec{i}}^r + \omega_{re}\mathbf{J}\vec{i}^r & \omega_{re}\begin{bmatrix}0\\1\end{bmatrix} \end{array}\right] \\ &= \left[\begin{array}{c|c|c} \tilde{i}_d^r & K_p e_{id}^r + \frac{d}{dt}\tilde{i}_d^r - \omega_{re} i_q^r & 0 \\ \hline \tilde{i}_q^r & K_p e_{iq}^r + \frac{d}{dt}\tilde{i}_q^r + \omega_{re} i_d^r & \omega_{re} \end{array}\right].\end{aligned} \tag{10}$$

It is assumed that the parameters are changing very slowly, i.e.,

$$\dot{\vec{e}}_\theta \approx -\dot{\hat{\vec{\theta}}} \tag{11}$$

where $\hat{\vec{\theta}} = \begin{bmatrix} \hat{R} & \hat{L} & \hat{\Lambda}_{PM} \end{bmatrix}^T$. Finally, the adaptive law is selected as,

$$\dot{\hat{\vec{\theta}}} = \mathbf{\Gamma}\mathbf{\Phi}^T\vec{e}_i^{\,r}, \tag{12}$$

and so (9) becomes

$$\dot{V}(\vec{e}_i^{\,r}, \vec{e}_\theta) = -\left(\frac{R}{L} + K_p\right)\vec{e}_i^{\,rT}\vec{e}_i^{\,r} \le 0. \tag{13}$$

Therefore, the closed-loop system (1), with control law (4) and adaptation (12), is stable in the sense of Lyapunov [13].

To establish asymptotic convergence of the stator current error (i.e., $\vec{e}_i^{\,r} \to 0$ as $t \to \infty$), we need to establish that $\dot{V}(\vec{e}_i^{\,r}, \vec{e}_\theta) \to 0$ as $t \to \infty$. This can be shown using Barbalat's lemma [13]. Note that the preceding Lyapunov

[1] $\{\cdot\}$ denotes a dynamic operator with transfer function ".".

Preprint submitted to 2014 American Control Conference.
Received September 27, 2013.

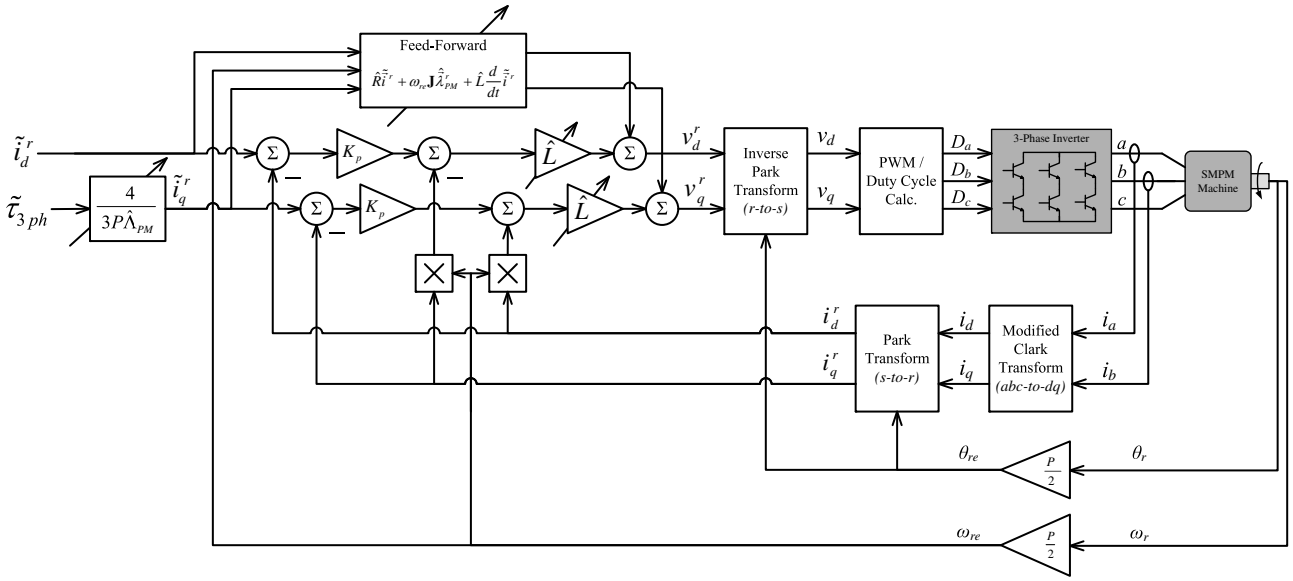

Fig. 2. Block diagram of the proposed control law.

stability analysis has established that $V(\vec{e}_i^{\,r}, \vec{e}_\theta)$ is differentiable and has a finite limit as $t \to \infty$. To establish uniform continuity of $\dot{V}(\vec{e}_i^{\,r}, \vec{e}_\theta)$ we compute,

$$\ddot{V}(\vec{e}_i^{\,r}, \vec{e}_\theta) = -2\left(\frac{R}{L} + K_p\right)\vec{e}_i^{\,rT}\dot{\vec{e}}_i^{\,r} \tag{14}$$

and note that

- $\vec{e}_i^{\,r}$ and $\vec{e}_\theta = [e_R \;\; e_L \;\; e_\Lambda]^T$ are bounded from (7) and (13),
- $\tilde{\vec{i}}^{\,r}$ and $\frac{d}{dt}\tilde{\vec{i}}^{\,r}$ are bounded by design, and
- $\vec{i}^{\,r} = \tilde{\vec{i}}^{\,r} - \vec{e}_i^{\,r}$ is bounded,

thus $\dot{\vec{e}}_i^{\,r}$ is bounded (from inspection of (6)), and so $\ddot{V}(\vec{e}_i^{\,r}, \vec{e}_\theta)$ is also bounded. Therefore, from Barbalat's lemma we have that $\dot{V}(\vec{e}_i^{\,r}, \vec{e}_\theta) \to 0$ as $t \to \infty$; and so we conclude that the control law (4) with adaptive law (12) renders the system (1) stable in the sense of Lyapunov with $\vec{e}_i^{\,r} \to 0$ as $t \to \infty$. Note that while the adaptive algorithm is derived in continuous-time, its experimental implementation is in discrete-time using a microprocessor.

IV. Sampled-Data Implementation

A. Time Delay and Compensation

The experimental implementation of the proposed control algorithm must take into account the sampled-data nature of its execution on a microprocessor. In particular, sampling of stator currents and encoder measurements is synchronized with a center-based pulse-width modulation (PWM) structure to prevent the pickup of electromagnetic interference (EMI) generated by switching transitions, during sampling. A consequence of this synchronization is that it leads to a one-switching-period delay between sampling measurements and updating duty cycles, as depicted in Fig. 3.

The presence of this time-delay will impose an upper limit on the proportional control gain, K_p. Additionally, the use of reference frame advancing in the inverse Park transform is

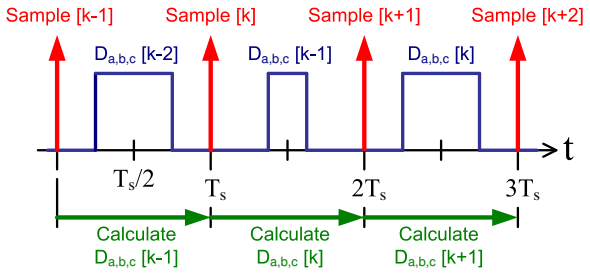

Fig. 3. Time sequence of digital controller implementation.

required as the rotor angular displacement during the delay interval can be significant. This discrepancy between the rotor position at the beginning and at the end of a sample period can lead to instability in the adaptive controller (Fig. 4).

To compensate for this angular displacement, the rotor position at the middle of the next sample period is predicted assuming that the rotor velocity is constant over the sample period, T_s:

$$\hat{\theta}_{re}[k+1] = \theta_{re}[k] + \frac{3}{2}\omega_{re}[k]T_s. \tag{15}$$

The predicted rotor position (15) is then used to compute the inverse Park transform in the discrete-time controller implementation. The inclusion of this simple predictor yields a stable closed-loop response (Fig. 5) when simulated with the same control gains, parameters, and initial conditions as the results in Fig. 4.

B. Switching σ-Modification for Robustness

As the simulation in the previous subsection demonstrated, adaptive laws such as (12) tend to lack robustness with respect to unmodeled time delays, dynamics and disturbances. It is therefore important to consider robust modifications to

Preprint submitted to 2014 American Control Conference.
Received September 27, 2013.

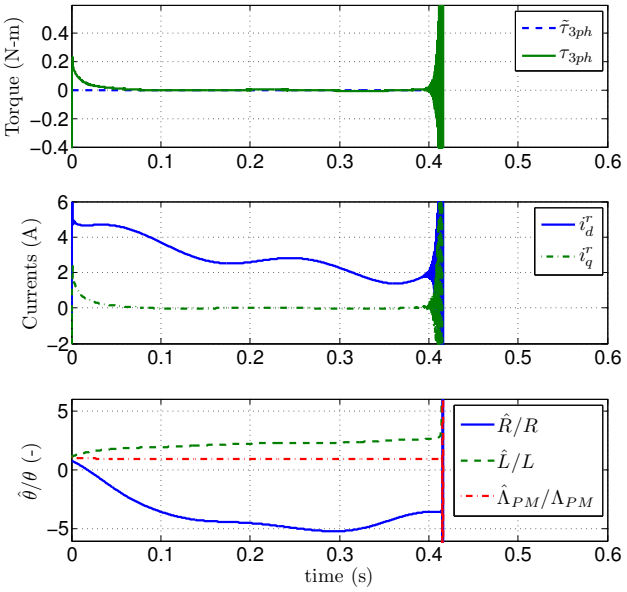

Fig. 4. Simulation of sampled-data system without reference frame advancing, leading to instability.

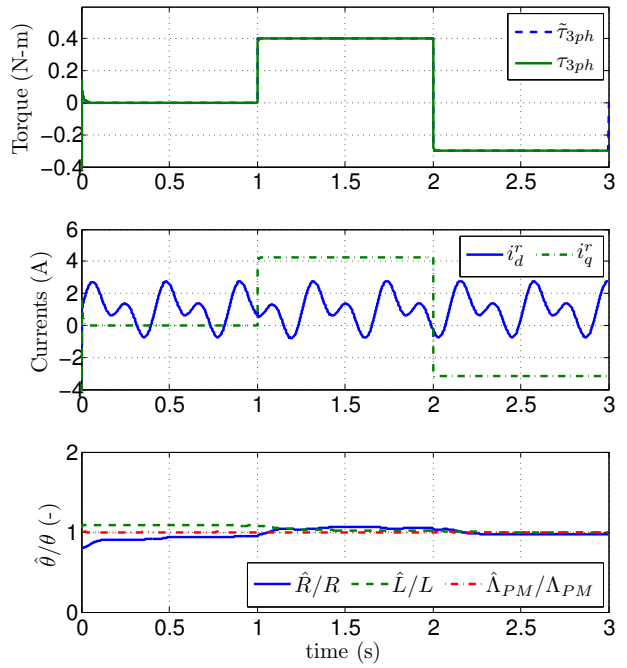

Fig. 5. Simulation of sampled-data system with reference frame advancing via angular rotor position prediction.

such adaptive laws. One such modification is the "switching σ-modification" [14] which acts as a "soft projection", applying a leakage term, σ, to the adaptive law only when a parameter is exceeding an expected limit on its range of variation. A benefit of this modification is that the ideal behavior of the adaptive law is preserved so long as the estimated parameters remain within their acceptable bounds (i.e., $|\theta(t)| < M_0$).

Including the switching σ-modification, our adaptive law becomes,

$$\dot{\hat{\vec{\theta}}} = \mathbf{\Gamma}\left(\mathbf{\Phi}^T \vec{e}_i^{\,r} - \sigma_0 \mathbf{\Sigma}_s \hat{\vec{\theta}}\right) \tag{16}$$

where

$$\begin{aligned} \mathbf{\Sigma}_s &= \text{diag}\left[\sigma_{s,1}, \sigma_{s,2}, \sigma_{s,3}\right], \\ \sigma_{s,i} &= \begin{cases} 0, & \text{if } |\hat{\theta}_i| < M_{0,i} \\ \frac{|\hat{\theta}_i|}{M_{0,i}} - 1, & \text{if } M_{0,i} \le |\hat{\theta}_i| \le 2M_{0,i} \\ 1, & \text{if } |\hat{\theta}_i| > 2M_{0,i} \end{cases} \\ i &= 1, 2, 3, \end{aligned} \tag{17}$$

with leakage parameter $\sigma_0 > 0$, and where $M_{0,i} > 0$ is the upper bound for the unknown parameter θ_i. This continuous switching function is depicted in Fig. 6. By choosing appropriate values for the design parameters σ_0 and $M_{0,i}$, parameter drifting due to bounded disturbances is prevented, ensuring stability of the closed-loop system.

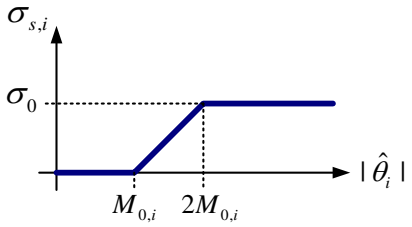

Fig. 6. Characteristic of switching σ-modification.

C. Ensuring Parameter Convergence

As the stability analysis demonstrated, the stator current error will always converge to zero at steady-state. However, convergence of the estimated parameter to their true values requires that the system is persistently excited (PE). While parameter convergence is not necessary to meet the control objective, having accurate knowledge of the machine parameters ensures that the desired transient response characteristics are maintained.

The simulation results presented in Fig. 7 demonstrate how commanding a PE direct-axis current ensures parameter convergence and that the desired transient characteristics are achieved. Additionally, ensuring parameter convergence allows the estimated parameters to be used for secondary objectives such as condition monitoring. An advantage of the proposed control design is that it permits the use of any persistently exciting direct-axis current command without disturbing the torque regulation.

V. Experimental Validation

A. Description of the Experimental Set-up

The proposed robust adaptive control algorithm has been implemented on experimental hardware using a dSPACE DS1104 controller board, and the test machine (Table III) is a 3-phase, 10-pole, 250 watt SMPM machine from MOTORSOLVER with "assumed" parameters (denoted by the over bar) listed in Table II. A 250 watt DC machine from

Preprint submitted to 2014 American Control Conference.
Received September 27, 2013.

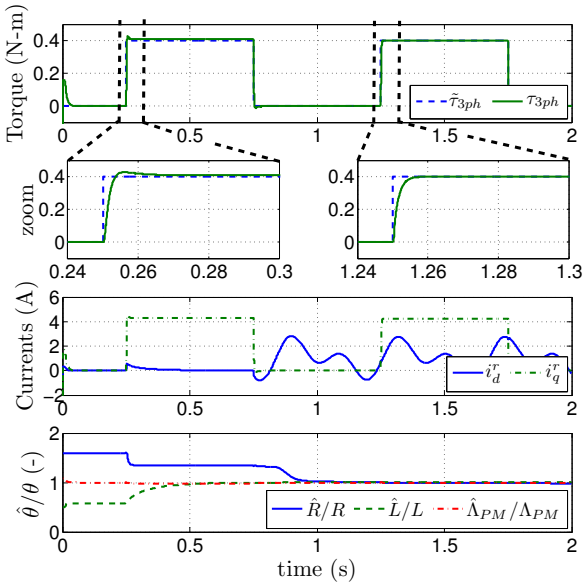

Fig. 7. Simulation results demonstrating the improvement in transient torque response (*see "zoom" subplot*) and parameter convergence with PE direct-axis stator current command (*turned "on" at t = 0.75 sec*).

TABLE III

MANUFACTURER MACHINE RATINGS.

Test Motor		Load Motor	
Type:	PM Brushless	Type:	DC
No. Phases:	3	No. Phases:	N.A.
V/I:	42 V/5.7 A	V/I:	42 V/6 A
Max. Speed:	4000 RPM	Max. Speed:	4000 RPM
Rated Power:	250 W	Rated Power:	250 W

the same manufacturer serves as the load for the SMPM machine.

A power MOSFET inverter is used to drive the motors with a switching frequency of 8 kHz and a bus voltage of 42 VDC. Duty cycles are calculated using Space Vector Modulation (SVM), and the ADC sampling is synchronized with, and offset from, the center-based PWM signals to avoid sampling during a switching event (as discussed in the previous section). The experimental setup is depicted in Fig. 8.

B. Experimental Results

Since mechanical torque was not measured during these experiments, the quadrature stator current (in the rotor reference frame) is used to evaluate the transient performance of the proposed torque regulator in addition to the estimated electromagnetic torque (18), which can vary with $\hat{\Lambda}_{PM}$:

$$\hat{\tau}_{3ph} = \frac{3P}{4}\hat{\Lambda}_{PM} i_q^r. \tag{18}$$

It should be noted that since torque cannot be measured directly, accurate knowledge of the PM flux linkage is required for accurate torque regulation. Online estimation of the PM flux linkage ensures that the desired electromagnetic torque will be obtained.

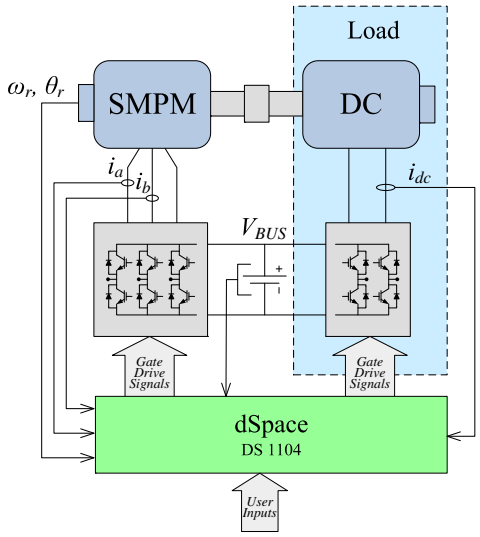

Fig. 8. Experimental setup.

A comparison of stator quadrature current responses for detuned ("Adaptation OFF") and tuned ("Adaptation ON") parameters is provided in Fig. 9. The detuned controller consists of the proposed control law (4) with the assumed machine parameters from Table II, and adaptation gains set to zero. Note that, while the detuned controller exhibits a mismatch in regulated variables, the tuned (adaptive) controller tracks the commands with zero average steady-state error.

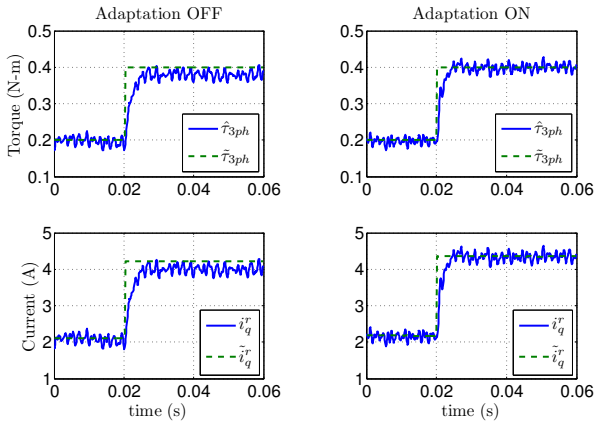

Fig. 9. Comparison of experimental transient responses for a torque step from 0.2 to 0.4 N-m at 2000 RPM.

Another feature of the proposed adaptive controller is that its closed-loop transient response remains consistent across a wide range of operating points. To demonstrate this, torque steps from 0 to 0.4 N-m were performed at 3000, 1500, and 0 RPM. These transient responses are provided in Fig. 10. Note that the responses overlay, indicating that the controller is performing as expected.

The transient response characteristics of the experimental adaptive parameter estimator for a constant torque command at a fixed rotor speed, are shown in Fig. 11. Note that the

Preprint submitted to 2014 American Control Conference.
Received September 27, 2013.

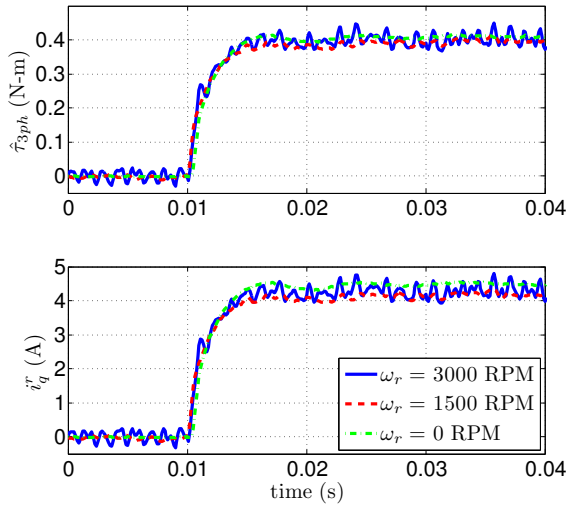

Fig. 10. Experimental transient responses of estimated torque (*top*) and measured quadrature-axis current (*bottom*) across a wide range of rotor speeds.

estimated parameter values, $\hat{\theta}$, have been normalized with respect to the "nominal" values, $\bar{\theta}$, in Table II. Additional excitation to aid parameter convergence was provided by commanding a sinusoidal direct stator current ($\tilde{i}_d^r = 1 + \sin(15t) + \sin(30t)$). The higher resistance and inductance were anticipated, as the parameters listed in Table II do not account for the additional resistance due to the $R_{DS,ON}$ of the MOSFET switches, the increase in resistance due to temperature and frequency, or errors in the RLC meter inductance measurement due to induced currents.

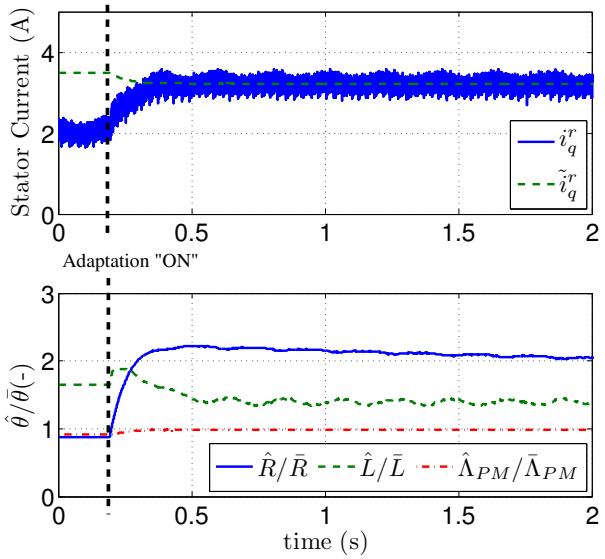

Fig. 11. Experimental adaptation parameter convergence for a constant 0.3 N-m torque command at 2000 RPM.

VI. Conclusion

This paper has presented a new robust adaptive torque regulating controller for SMPM machines which concurrently estimates resistance, inductance, and permanent magnet flux linkage online. The closed-loop stability of the controller was demonstrated in the process of its derivation using Lyapunov stability theory. Simulation results confirm the performance of the proposed adaptive control design, and experimental results validating the algorithm over a wide operating range were presented.

References

[1] R. Krishnan, *Permanent Magnet Synchronous and Brushless DC Motor Drives*. Boca Raton: CRC Press, 2010.

[2] B. Bose, *Modern Power Electronics and AC Drives*. New Jersey: Prentice Hall PTR, New Jersey, 2002.

[3] F. Blaschke, "The principle of field orientation as applied to the new transvector closed loop control for rotating field machines," *Siemens Rev.*, vol. 39, pp. 217–220, May 1972.

[4] R. Park, "Two-reaction theory of synchronous machines, generalized method of analysis - part 1," *A.I.E.E. Transactions*, vol. 48, pp. 81–95, 1929.

[5] S. Underwood and I. Husain, "Online parameter estimation and adaptive control of permanent-magnet synchronous machines," *IEEE Transactions on Industrial Electronics*, vol. 57, pp. 2435 – 2443, July 2010.

[6] S. Ichikawa, M. Tomita, S. Doki, and S. Okuma, "Synchronous motors using online parameter identification based on system identification theory," *IEEE Transactions on Industrial Electronics*, vol. 53, pp. 363 – 372, April 2006.

[7] R. Delpoux, M. Bodson, and T. Floquet, "Parameter estimation of permanent magnet stepper motors without position or velocity sensors," *Proceedings of the 2012 American Control Conference*, pp. 1180 – 1185, 2012.

[8] Y. A.-R. I. Mohamed, "Design and implementation of a robust current-control scheme for a pmsm vector drive with a simple adaptive disturbance observer," *IEEE Transactions on Industrial Electronics*, vol. 54, pp. 1981 – 1988, August 2007.

[9] K. Liu, Q. Zhang, J. Chen, Z. Zhu, and J. Zhang, "Online multi-parameter estimation of nonsalient-pole pm synchronous machines with temperature variation tracking," *IEEE Transactions on Industrial Electronics*, vol. 58, pp. 1776 – 1788, May 2011.

[10] L. Liu and D. Cartes, "Synchronisation based adaptive parameter identification for permanent magnet synchronous motors," *IET Control Theory Applications*, vol. 1, pp. 1015 – 1022, July 2007.

[11] H. Kim and R. Lorenz, "Improved current regulators for ipm machine drives using on-line parameter estimation," *Conf. Rec. IEEE-IAS Annual Meeting*, vol. 1, pp. 86 – 91, 2002.

[12] K.-W. Lee, D.-H. Jung, and I.-J. Ha, "An online identification method for both stator resistance and back-emf coefficient of pmsms without rotational transducers," *IEEE Transactions on Industrial Electronics*, vol. 51, pp. 507 – 510, April 2004.

[13] J.-J. E. Slotine and W. Li, *Applied Nonlinear Control*. New Jersey: Prentice Hall, 1991.

[14] P. Ioannou and J. Sun, *Robust Adaptive Control*. New Jersey: Prentice Hall, 1996.

Preprint submitted to 2014 American Control Conference.
Received September 27, 2013.